Overview of RFX-mod results

P. Martin 1), L. Apolloni 1), M. E. Puiatti 1), J. Adamek 2), M. Agostini 1), A. Alfier 1), S.V. Annibaldi 3), V. Antoni 1), F. Auriemma 1), O. Barana 1), M. Baruzzo 1), P. Bettini 1), T. Bolzonella 1), D. Bonfiglio 1), F. Bonomo 1), M. Brombin 1), J. Brotankova 2), A. Buffa 1), P. Buratti 3), A. Canton 1), S. Cappello 1), L. Carraro 1), R. Cavazzana 1), M. Cavinato 1), B.E. Chapman 5), G. Chitarin 1), S. Dal Bello 1), A. De Lorenzi 1), G. De Masi 1), D. F. Escande 1,6), A. Fassina 1), A. Ferro 1), P. Franz 1), E. Gaio 1), E. Gazza 1), L. Giudicotti 1), F. Gnesotto 1), M. Gobbin 1), L. Grando 1), L. Guazzotto 1), S. C. Guo 1), V. Igochine 7), P. Innocente 1), Y.Q.Liu 8), R. Lorenzini 1), A. Luchetta 1), G. Manduchi 1), G. Marchiori 1), D. Marcuzzi 1), L. Marrelli 1), S. Martini 1), E. Martines 1), K. McCollam 5), F. Milani 1), M. Moresco 1), L. Novello 1), S. Ortolani 1), R. Paccagnella 1), R. Pasqualotto 1), S. Peruzzo 1), R. Piovan 1), P. Piovesan 1), L. Piron 1), A. Pizzimenti 1), N. Pomaro 1), I. Predebon 1), J.A. Reusch 5) G. Rostagni 1), G. Rubinacci 9), J. S. Sarff 5), F. Sattin 1), P. Scarin 1), G. Serianni 1), P. Sonato 1), E. Spada 1), A. Soppelsa 1), S. Spagnolo 1), M. Spolaore 1), G. Spizzo 1), C. Taliercio 1), D. Terranova 1), V. Toigo 1), M. Valisa 1), N. Vianello 1), F. Villone 10), D. Yadikin 7), P. Zaccaria 1), A. Zamengo 1), P. Zanca 1), B. Zaniol 1), L. Zanotto 1), E. Zilli 1), H. Zohm 7), M. Zuin 1)

1) Consorzio RFX, Associazione EURATOM-ENEA sulla Fusione, 35137 Padova, Italy
2) Institute of Plasma Physics, Association EURATOM-IPP.CR, Prague, Czech Republic
3) Space and Plasma Physics, EE KTH, SE-10044 Stockholm, Sweden
4) Associazione Euratom-ENEA sulla Fusione, C.R. Frascati, 00044 Frascati, Roma, Italy
5) Department of Physics, University of Wisconsin, Madison, WI, USA
6) UMR 6633 CNRS-Université de Provence, Marseille, France
7) Max-Planck-Institut für Plasmaphysik, EURATOM Association, 85748 Garching, Germany
8) EURATOM-UKAEA Fusion Ass., Culham Science Centre, OX14 3DB, Abingdon, OXON, UK
9) Ass. Euratom/ENEA/CREATE, DIEL, Università di Napoli Federico II, Napoli, Italy
10) Ass. Euratom/ENEA/CREATE, DAEIMI, Università di Cassino, Cassino, Italy

e-mail contact of main author: piero.martin@igi.cnr.it

Abstract. With the exploration of the MA plasma current regime in up to 0.5 s long discharges, RFX-mod has opened new and very promising perspectives for the Reversed Field Pinch (RFP) magnetic configuration, and has made a significant progress in understanding and improving confinement and in controlling plasma stability. A big leap with respect to previous knowledge and expectations on RFP physics and performance has been made by RFX-mod since the last 2006 IAEA Fusion Energy Conference. A new self-organised helical equilibrium has been found (the Single Helical Axis – SHAx – state), which is the preferred state at high current. This regime is characterized by strong core electron transport barriers, with electron temperature gradients comparable to those achieved in tokamaks, and by a factor four improvement in confinement time with respect to the standard RFP. RFX-mod is also providing leading edge results on real-time feedback control of MHD instabilities, of general interest for the fusion community.

1. RFX-mod: mission, results, and challenges

RFX-mod [1] is the largest reversed field pinch (RFP) device and it is capable of achieving the highest plasma current. It is based in Padova, Italy and its major and minor radii are R=2 m and a=0.459 m respectively, for a plasma volume of about 10 m^3. The maximum design plasma current is 2 MA, which allows exploring current regimes comparable to those of large tokamaks, but with a toroidal magnetic field ten times smaller.
RFX-mod is the renewed and upgraded version of the former RFX device, and started its operation in December 2004. The original RFX thick shell (which had a magnetic field

penetration time constant τ_{shell}=500 ms) was replaced with a thinner one, whose time constant for penetration of vertical magnetic field ($\approx$50 ms) is $\approx$10 times shorter than pulse duration. Moreover, RFX-mod is equipped with the most advanced system for feedback control of MHD stability with active coils ever realized in a fusion device. The system is based on 192 active saddle coils, which cover the whole plasma boundary. The coils are arranged in 48 toroidal locations; in each toroidal location there are 4 poloidal coils, according to the low m/high n structure of MHD modes in the RFP (where m and n are the poloidal and toroidal mode number respectively). Each coil is independently driven by individual power supplies and can produce a radial magnetic field up to 50 mT DC and 3.5 mT at 100 Hz. A set of 576 signals is acquired and processed in real-time [2]. This set includes 192 components of both radial and toroidal magnetic field and 192 saddle coil current measurements. The real-time software has been highly optimized to maximize the sampling frequency (2.5 kHz) and minimize the cycle latency ($\leq$ 400 μs). An integrated, distributed, digital control system [2] includes, so far, seven computing nodes exchanging data during operation via a real-time network.

The RFP is one of the two most developed alternatives to the tokamak, and in a complex and goal-oriented programme like fusion it contributes by providing elements of diversity and flexibility, to proceed faster, prevent risk, increase predictive capability by exploring the widest parameter range. The RFP: a) may provide an alternative reactor concept, possibly technologically easier in some respects, b) contributes to the understanding of tokamak physics, in particular stretched at the extreme of low magnetic field, c) contributes to the solution of technology problems for ITER (and the RFP community is presently the leading one in the area of active control of MHD stability with coils).

In this framework, during the last decade, significant results have been accrued. In particular, experimental and theoretical results induced a change of paradigm. Multiple MHD instabilities are not anymore considered an essential ingredient of the RFP dynamics, as it happened in the standard Multiple Helicity (MH) configuration. Indeed, experiments in present generation devices back up the new theoretical understanding; the basic nature of the system can be described as a self-organized helical state corresponding to the nonlinear saturation of a kink-tearing mode, called the dominant mode. This is the Single Helicity – SH – state [3]. The existence of RFP equilibrium with perfectly conserved helical confining magnetic surfaces is clearly extremely important for confinement, and overturns the old paradigm of the RFP as dominated by magnetic chaos. This is at variance with the previous traditional idea of the RFP as a relaxed axis-symmetric state, which, by theoretical arguments, requires the action of turbulence to accomplish and to maintain relaxation

Since the last Fusion Energy Conference in 2006, RFX-mod has made impressive progresses: with the exploration of the MA current regime in discharges up to 0.5 s long, a new self-organised helical equilibrium has been found (the Single Helical Axis – SHAx – state), which is the preferred state by the plasma at high current. This regime is characterized by strong core electron transport barriers, with electron temperature gradients comparable to those achieved in the tokamak, and by a factor four improvement in confinement time with respect to the standard RFP. These findings open new and very promising fusion perspectives for the configuration. Moreover, RFX-mod is participating to the world-wide effort for ITER, and provides an excellence pole for the studies on plasma stability real-time control, with leading edge results. In particular, the MHD stability control system has been improved, which allows efficient multi-mode control both for tearing and resistive wall modes (RWM). Moreover, the availability of a broad experimental database allowed to benchmark against measurements the CarMA code, designed to predict MHD stability in ITER in presence of 3-d boundary structures.

The paper is organized as follows: Sect. 2 is dedicated to MHD stability real-time control, and the most import results on tearing modes, resistive wall modes and control engineering and modeling are discussed. Sect. 3 describes the outcome of the high current campaign (up to 1.6 MA), with the impressive results on confinement improvement and spontaneous self-organization towards helical states. Sect. 4 illustrates the progress on understanding the Greenwald density limit, while Sect. 5 is focused on fundamental studies on turbulence driven transport.

2. MHD stability real-time control

2.1. Control of resistive tearing modes

At the time of the 2006 FEC, the Virtual Shell (VS) control scheme was implemented [2]. In VS the flux through each sensor loop is controlled by the corresponding active coil. This scheme corresponds to the Intelligent Shell approach [4]. Compared to passive operations, VS allowed significant improvements in plasma performance [5,6], but a careful analysis revealed that the action of the VS on the edge value of the tearing modes is limited by a systematic error: the measured magnetic field harmonics includes the aliasing of the high poloidal and toroidal mode number sidebands [7] produced by the discrete coils grid. Basically, the VS successfully cancels the measurements of the edge radial field, but not necessarily all its Fourier harmonics. Another important source of systematic error in the feedback is due to the radial distance between the sensor coils (located at $r=0.507$ m) and the plasma edge ($r=0.459$ m). The radial field at the plasma edge is significantly higher than the field at the sensor radius. Therefore, without correction, even a perfect cancellation of the radial field at the sensors does not imply that the field is zero at the plasma edge. Both processes may leave a significant amount of edge radial perturbation.

A cleaning and extrapolation algorithm, dubbed Clean Mode Control (CMC) has been developed to remove the aliasing of sidebands from the measurements [8] and is presented at this Conference [9]. As the sensors are inside the thin shell, while the active coils are outside, each sideband penetrates with a different time constant: a dynamical model is required.

The cleaned harmonics, extrapolated to the plasma edge, are finally used as feedback variables and the digital controller determines the feedback reaction with a PID approach.

The cleaning and the extrapolation algorithms have then been implemented in real-time, requiring a significant upgrade of the real-time feedback system architecture [10]. The corrections need, in fact, the real-time acquisition of 48x4 saddle coil current and 48x4 toroidal field sensors and their processing in the same real-time node. A new node, the Coil Current Processor, has been implemented, with the corresponding introduction of 192 additional control analogue input signals (from 544 to 736). The clock frequency
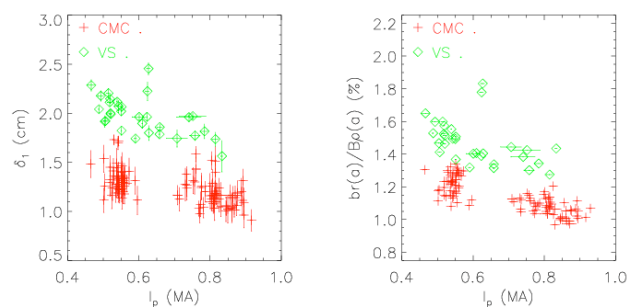

Fig. 1: a) δ_1 vs. plasma current CMC discharges (red dots), standard VS discharges (green diamonds). b) Quadratic sum of the m=1 radial field at the edge, normalized to the equilibrium poloidal field.

of the PowerPC-based central processing units was upgraded from 500 to 1000 MHz and their communication ports from 100 to 1000 MByte/s.

CMC has many positive effects [9]. First of all, a lower value of the edge radial field is obtained and, as a consequence, the localized non-axisymmetric displacement of the Last Closed Magnetic Surface, δ_1, is strongly reduced (Fig. 1).

Differential rotation of the tearing modes up to 100Hz is induced. Phase locking is then considerably mitigated and wall-locking is avoided. This leads to a much cleaner magnetic boundary and to a dramatically reduced plasma-wall interaction. Heat loads are spread around the first wall during each discharge and they are not toroidally localized as it happened in VS [9,11]. These are conditions that, as shown in Sect. 3, favour the appearance of helical states.

2.2. Resistive wall modes physics and control

Optimal feedback control of resistive-wall modes (RWM) is of common interest for tokamak

and RFP. The RFP situation is similar to the advanced tokamak in presence of very low plasma rotation, where the most effective stabilizing mechanism is the feedback action of active coils. Already at the 2006 FEC it was reported the full stabilization of multiple RWMs in RFX-mod [5,6]. Dedicated experiments on RWM physics and control are presented at this Conference [12]. An example is selective control of one or more RWMs in order to study their mutual interactions and their interactions with the bulk plasma or with other MHD instabilities. This is shown in Fig. 2 where the growth rate of a selected unstable RWM is modified by using a range of different proportional gains to simulate the effect of control systems with different power capabilities (an issue definitely important for new devices, like ITER).

Figure 2: Proportional gain scan on the (1,-6) RWM. Increasing gain values follow the colors from green (lower gain) to black (higher gain).

Optimized control schemes allow to address fundamental ITER relevant MHD physics issues, like the question of how the flow velocity of the background plasma influences the MHD stability. This is the subject of a collaboration with ASDEX-Upgrade [13].

The relative rotation of fluid plasma and MHD instability has been changed by directly acting on the mode itself. This approach is complementary to the one aiming at studying the RWM stabilization by plasma rotation either braking the plasma with external field errors [14] or changing its flow velocity with differently balanced tangential injection of momentum [15,16]. Initially a RWM is kept at finite amplitude by means of a suitable proportional gain (partial control). Then a small imaginary gain is added to the proportional gain. In this way the external feedback action has a phase difference with respect to the plasma mode and reacts to keep it constant. Experimental results are shown in Fig. 3 for the (m=1, n=−6) mode and indicate that finite amplitude RWMs can be detached from the resistive wall and put in rotation by the action of the external control system with a phase velocity that depends only on the phase
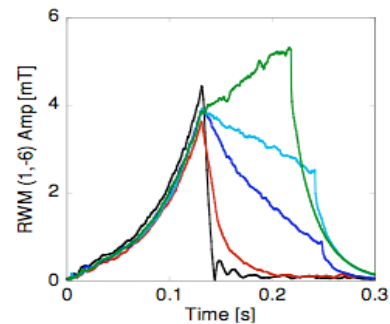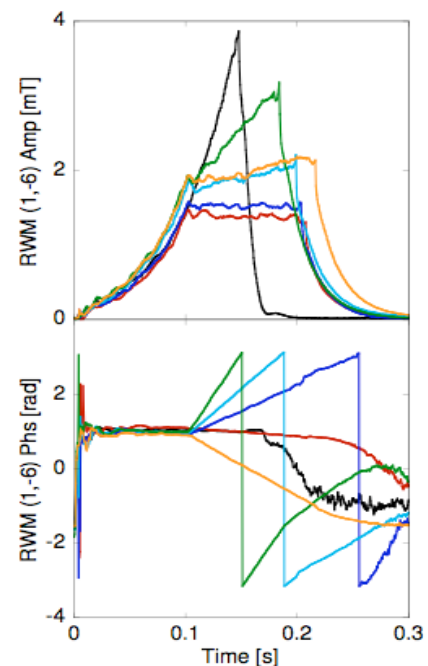

Fig. 3: Imaginary gain scan on the (1,-6) RWM. (top) mode amplitudes, (bottom) mode phases. Black full traces represent a reference shot where (1,-6) RWM is initially free to grow and later in the discharge fully controlled. Other colors correspond to the application of finite imaginary gain gains: the RWM rotation can be induced in both opposite directions (feedback in action from 0.1s).

difference between the mode and the external perturbation. Plasma rotation, current and coupling to other modes have no impact on the rotation frequency.

Accurate modeling of MHD stability and control is a key request for ITER. This requires understanding the effects on stability of plasma rotation and of the complex 3-d conducting structures surrounding the plasma. Since RWM stability in RFP is not affected by dissipation and flow, the RWM modelling can focus on the analysis of 3-d effects removing other sources of uncertainties. To this purpose, a collaboration between the RFX-mod, UKAEA, and CREATE implemented a 3-d model of RFX-mod in the new code CarMa [17]. CarMa rigorously takes into account the 3-d details of the conducting structures, and accounts for multiple toroidal Fourier harmonics in the plasma response. CarMa predictions have been benchmarked against RFX-mod experimental data for the first time, which is very useful for its applications to ITER [18]. The CarMa RWM growth rates have been compared with RFX-mod data, and with the predictions of

TABLE I: Comparison between numerical and experimental RWM growth rates.

	ETAW	MARSF	CarMa	Exp.
$n=4$	5.27	5.07	7.30 7.48	≈ 6
$n=5$	8.63	8.55	12.8 13.1	≈ 12
$n=6$	14.5	14.4	22.6 23.4	≈ 22

the cylindrical code ETAW and of the toroidal MHD code MARS-F [18]. Some of the results are presented in Table I and show a clear improvement when 3-d boundary effects are taken into account. They may play a significant role in RWM stability with direct implication to ITER predictions.

2.3. Advancements in control theory and implementation

While the control system is based on a significantly high number of sensors and actuators, the control schemes used so far, i.e. both the VS and the CMC, are based on a Single Input Single Output (SISO) approach, i.e. the feedback law considers only one input (a sensor measurement in VS or a discrete Fourier harmonic in CMC). This SISO approach does not take into account the couplings between the actuators and the sensor coils. To go beyond the SISO scheme a Multiple Input Multiple Output (MIMO) control system is being implemented, which considers in each feedback law multiple inputs to take into account the coupling with neighbour coils.

The design of the MIMO controller is based on a model of the electromagnetic system, including coils, sensors and passive structures [10]. This model simulates the sensor measurements generated by the actuator coils. A first attempt uses the Dynamic Pseudo Decoupler control scheme [19], which is a generalization of the decoupling matrix concept [2]. An alternative approach is being developed, which considers the couplings between discrete Fourier harmonics of sensor signals and actuator coils. In fact, the toroidal geometry and the presence of gaps in the shell and the support structure cause a non-negligible coupling between different harmonics with the same toroidal modes and different poloidal number. Undesired modes and associated sidebands are unavoidably produced together with the targeted ones. They can excite plasma modes via error field amplification, and may cause additional power consumption.

Both approaches highlighted the requirement of a more accurate model of the electromagnetic system. Such a model was, in fact, experimentally identified only for a subset of the coils and the missing mutual couplings were defined by assuming symmetry. No knowledge about the sensors or actuator coils geometry is assumed. In order to improve the model two actions were undertaken. First, new measurements were acquired for a sample of coils and, secondly, the finite element code CARIDDI [17] was used to provide calculated "virtual measurements" where they are missing or noisy. In particular measurements are used to refine the 3-d representation of the RFX passive structures used by CARIDDI [20].

3. High current operation, self-organized helical equilibria and improved confinement.

3.1 The 1.6 MA scenario

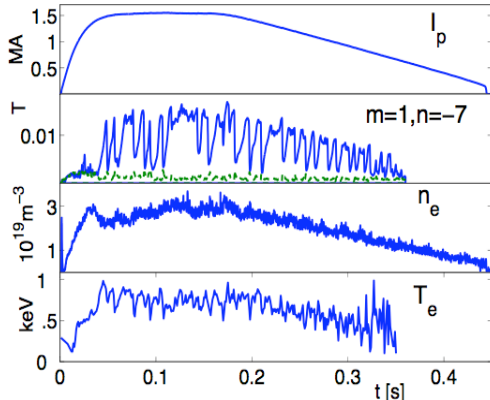CMC provides robust improvements in the quality of the magnetic boundary and in the level of plasma-wall interaction, so that old problems like mode locking or localized interactions are mostly solved. As a result, operation up to record current level of 1.6 MA is routinely and reliably carried out [21]. Plasma discharges as long as approximately 0.5 s (i.e. several times the resistive wall constant) are produced, thus demonstrating that the RFP does not need for its operation a thick conductive shell. A typical plasma current discharge in RFX-mod is illustrated in Fig. 4, which displays some relevant time traces (see caption). The plasma current is sustained by static units till t=150 ms. During the long decay only the vertical and the edge magnetic fields required to keep a prescribed edge safety factor are actively controlled.
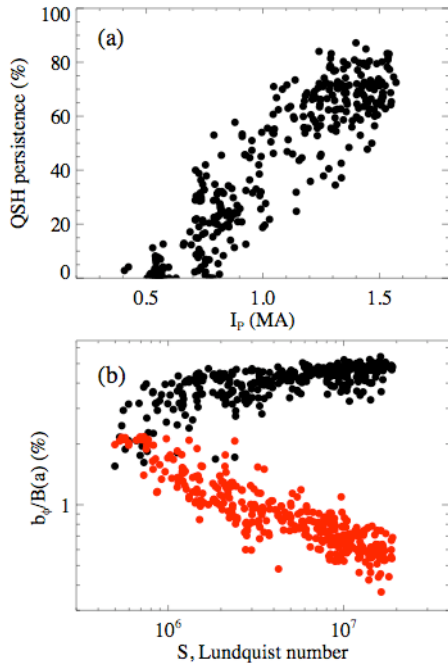
High current operation lead to dramatic changes: for the first time a robust and persistent self-organization towards a chaos-free ohmic helical equilibrium, with strong transport barriers and improved confinement properties, is observed. This happens thanks to the natural tendency of RFP plasma to move, when plasma dissipation changes, towards a single helicity condition, that is a condition where only one of the core-resonant tearing modes provides the dynamo effect [22].

As shown in Fig. 4, after the setting-up phase, the innermost resonant resistive kink mode (m=1, n=−7) becomes higher than all the other secondary modes (m=1, $|n|\geq 8$), which instead decrease. This gives a strong and tidy helical character to the magnetic topology, where one m=1 mode is dominant in the tearing mode k spectrum. This is the present best approximation of the SH state (Quasi Single Helicity – QSH). This QSH state is not fully stationary, yet: phases where the amplitude of the dominant mode persists high up to tens of ms (up to 50 ms), that is several times the energy confinement time, are interrupted by occasional crashes of the dominant mode to lower values, still higher than the amplitude of the remaining secondary modes [21].

Fig. 4: Time traces for discharge #24063. From top: Plasma current; Amplitude of m=1 n= -7 and (dashed line) average amplitude of "secondary" modes m=1 n=- 8/-14; electron density and electron temperature.

Fig. 5: (a) Persistency of the QSH state vs. plasma current. Persistency is defined as the fraction of the plasma current flat-top featuring a QSH. (b) scaling of dominant mode and secondary mode average amplitude vs. the Lundquist number S.

Long lasting QSH periods are more probable as plasma current increases. This is shown in Fig. 5-a, where the QSH persistency is reported as a function of the plasma current for a large number of discharges. This behavior is correlated with the general scaling of the magnetic fluctuation amplitude vs. the magnetic Lundquist number S, defined as $S = \dfrac{30 I_\phi Te(0)^{3/2}}{z_{eff} \lg \Lambda \sqrt{m_i n_e}}$.

The amplitude of the dominant (m=1,n=-7) mode and that of the secondary modes scale in opposite ways with S: while in the explored S range the dominant mode increases, initially faster and than in a slower fashion, the secondary mode amplitude continuously decreases, as shown in Fig. 5-b. This two opposite scalings work synergistically to improve the quality of magnetic surfaces, and then of plasma confinement, at the higher values of S, which in the present database correspond to the higher plasma current. In fact the helical core, driven by the amplitude of the (m=1,n=-7) mode, grows larger while the overall magnetic chaos outside it, driven by the amplitude of the secondary modes, decreases.

3.2 Self-organized helical equilibrium
Two main categories of helical states are observed depending on the relative amplitude of the dominant mode: (1) that where a helical structure is present, but the plasma maintains its axisymmetric magnetic axis together with the secondary magnetic axis. In this case the helical
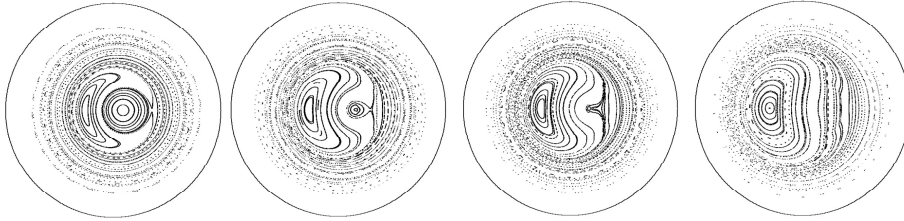

Fig. 6: The Poincaré plots are obtained considering only the axisymmetric field and the dominant perturbation.

structure is bounded by a magnetic separatrix. (2) That where the dominant m=1 mode grows up to the point where its helical axis becomes the main magnetic axis, and the original symmetric magnetic axis ceases to exist. These type 2 helical states correspond to the helical equilibrium theoretically predicted [23], which is expected to be more resilient to magnetic chaos. Fig. 6 shows how the plasma magnetic flux surfaces change passing from a state with separatrix to one without. Helical states without separatrix, dubbed Single Helical Axis (SHAx) states, have been first observed driven by the Oscillating Poloidal Current Drive (OPCD) technique [24]. Now the important novelty is that they appear as a natural and preferred outcome of the high current operation. This regime is the closest ever achieved to the predicted Single Helicity regime.

The synergistic S scalings have important consequences for the quality of magnetic confinement, as discussed in [25]. In fact when the dominant mode amplitude, normalized to the edge magnetic field, is larger than $\approx$ 4%, all QSH states become SHAx. In SHAx states the positive features of the QSH states with separatrix are greatly amplified. In fact, when the separatrix is present in a QSH state, electron temperature profiles display a strong and local temperature peak, associated with the island located at the mode resonant surface. This peak extends throughout the island width (corresponding to approximately 10 – 20 % of the plasma major diameter). Though peak temperature might be rather high (up to 1.2 keV to now) and steep gradients are present ($1/L_{Te}$ of the order of 20 m^{-1} is measured), the overall effect on confinement is not very large since the volume occupied by the well confining helical surfaces is only $\approx$ 10-20% of the total plasma volume. The situation in the SHAx states is rather different: the expulsion of the separatrix by the dominant mode leaves a relatively large structure of nested helical magnetic surfaces, resilient to the influence of surviving secondary modes. As a result, electron temperature profiles show strong electron transport barriers, which extend further than 0.5 r/a and bound a large fraction of the plasma.

Two sample profiles from the two QSH categories are shown in Fig.7, which also shows the corresponding magnetic surfaces. Electron temperature and density profiles and the 2-d map of SXR emissivity are key elements to prove that in SHAx states helical magnetic surfaces actually exist, and therefore that these states correspond to an equilibrium, though not

stationary, yet. An effective method for computing the helical flux $\psi(r)$ and therefore the shape of the magnetic surfaces for the SHAx state has been developed, based on the assumption that the magnetic field can still be written as the superposition of an axisymmetric equilibrium and of the helical modulation corresponding to the dominant $m=1$ mode eigenfunction [26]. If these surfaces are not destroyed by magnetic field chaos, flux functions should be constant on them. In particular, this applies to kinetic pressure. In RFX-mod the density profile close to magnetic axis is typically flat. Thus, one expects temperature to be a flux function in the plasma core. Fig. 8-a shows a typical SHAx electron temperature profile plotted as a function of the effective radius $\rho = (\psi/\psi_0)^{1/2}$, where ψ_0 is the helical flux at the plasma boundary. The two half profiles measured on the two sides
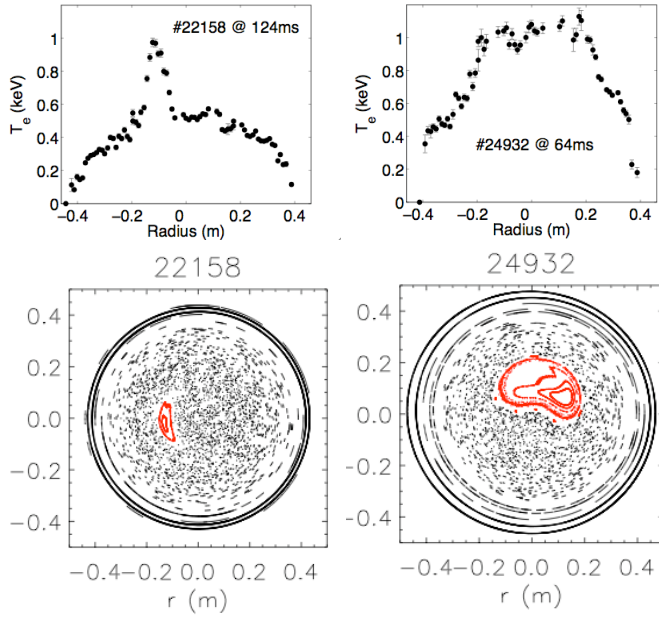
Fig. 7: electron temperature profiles and magnetic surfaces for a QSH state with separatrix (left column) and without (SHAx, right column). Poincaré plots are taken at the toroidal location where the electron temperature profile is measured. Even if it is not visually evident, the level of magnetic chaos in the SHAx plasma core is strongly reduced, with magnetic field lines being more sticky and much less prone to wander from core to edge.

of the geometric axis, marked by different colours, collapse on each other when plotted as a function of ρ. In particular, the gradients turn out to be the same. A reconstruction of the 2D map of the temperature on the poloidal plane is shown in Fig. 8-b. The hot region is bean-shaped, and centred off the geometric axis, on the resonant surface of the $m=1/n=-7$ mode. With the same method the analysis of soft x-ray (SXR) tomographic data and of density profile during pellet injection provides a further confirmation that the computed helical flux surfaces are isothermal and isoemissive surfaces.

3.3 Transport and confinement in the helical state: status and perspectives
Electron thermal conductivity χ_e profiles are consistent with the strong transport barriers, and record values for χ_e lower than 20 m^2/s are measured, as shown in Fig. 9.
In SHAx regimes magnetic driven transport could be so small that drift modes, of electrostatic nature, may become important. Both gyrokinetic and fluid approaches have been adopted to study Ion Temperature Gradient (ITG) modes in RFP plasmas. The result is that these instabilities are in general more stable in a RFP than in a tokamak, due to the shorter connection length in RFP, but can be excited in the regions where very high T_e gradients are present, namely at the edge of the islands associated to a QSH and at the edge of the plasma [27]. Ion temperature profile measurements are not available on RFX-mod yet. Line of sight integrated Doppler broadening measurements on OVIII, OVII, CV and simulation of impurity emission profiles indicates that $T_i \sim (0.6\text{-}0.7)\,T_e$: T_i profile measurements will clarify if the scenario of a RFP core dominated by electrostatic instability is consistent. This would be a change of perspective for the RFP physics. Other numerical tools developed to study drift turbulence in tokamak such as TRB [28] and GS2 [29] are also being adapted to investigate RFP plasmas.

The higher degree of magnetic order in SHAx equilibria results also in a more ordered plasma-wall interaction [9,11]. This is confirmed by measurements of floating potential, total radiation, H_α emission. During the SHAx states a $|n| = 7$ spatial modulation of the plasma-wall interaction is visible.

Experimental evidence [25] indicates a different behavior between impurities and main gas diffusion mechanisms in QSH: transport of main gas appears to be decreased by QSH, while impurity transport seems not to depend on the presence of QSH. This might be a positive indication in terms of avoidance of impurity accumulation issues in advanced RFP states.
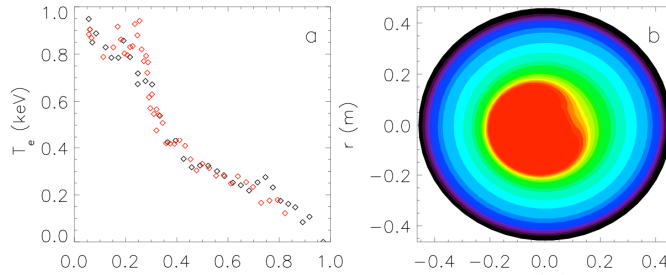

Figure 8: typical SHAx electron temperature profile and reconstruction of the 2D map of the temperature on the poloidal plane
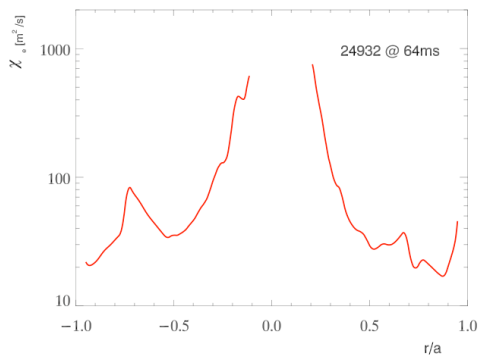
Up to now high performance SHAx states have been obtained with electron densities normalized to the Greenwald density, n/n_G typically below $n/n_G= 0.3$. In this range confinement increases linearly with density for any given current. *Electron* energy confinement time increase on the average by a factor of ≈ 2 in QSH states with separatrix with respect to MH states. In SHAx states an additional factor of ≈ 2 is gained, which leads to an overall gain by a factor of ≈ 4 with respect to standard RFP plasmas. Best *electron* energy confinement values τ_{Ee} in stationary conditions at $n/n_G < 0.3$ are around 2 ms. This should be compared with the best values ≈ 0.7 ms reported at the last FEC [30] at 1 MA (the highest current reached at that time), and indicates a substantial progress. If $T_i=T_e$ then the global energy confinement time is $\tau_E=2\tau_{Ee}$. At the moment there is an issue with operation at high n/n_G, where the density profiles tends to become hollow and the plasma is more resistive.

Fig. 9: heat conductivity profile for the SHAx state in #24932, 64 ms (corresponds to the T_e profile of Fig.7). In the region around r/a=0 the T_e profile is flat and χ_e is not defined)

Operational conditions on low wall recycling become more stringent. The problem should be solved with appropriate wall-conditioning (boronization and, in the future, lithization) and with fuelling by pellet injection. Initial experiments to inject pellets into high current low density target plasmas have started. Peaked density profiles, with refueling of the helical core, and record values of *electron* energy confinement times τ_{Ee} between 2.5 and 3 ms are obtained transiently. This appears promising to achieve advanced regimes at high density, with an additional improvement of the confinement performance.

4. Density limit

Several elements to improve the understanding of the Greenwald density limit, which shares many features with the tokamak, has been provided by RFX and are discussed in [31] presented at this conference. The RFP operating space is limited at high density by the Greenwald empirical law, as in the tokamak. In RFX-mod such limit has been experimentally characterized [31], suggesting a clear relation with the $m=0$ toroidally localized structures generated by the non-linear interaction among the $m=1$ modes. When density approaches the Greenwald value, a radiating belt is observed, poloidally symmetric and toroidally localized in

the region where, due to the $m=0$ mode, the plasma shrinks. Correspondingly, the impurity line radiation increases and the plasma edge cools down. At the same toroidal position the density increases and peaks at the edge, where it becomes about twice than in the core. Such density accumulation does not correspond to a local enhancement of the source and may be interpreted as a combined effect of plasma flow inversion and edge transport dependence on density. Measurements of the toroidal velocity show that the flow changes sign where the local radial magnetic field is positive. Particles, that are mainly produced and diffused into the plasma where in MH $m=1$ modes are locked and the PWI is stronger, are toroidally conveyed towards a stagnation point, corresponding to the region of plasma shrinking. Here they can accumulate, due to the decreasing dependence of the plasma diffusivity on density [11] and to a radial flux lower than the toroidal convection [31]. The phenomenology of the radiating belt recalls that of MARFES, observed both in tokamaks and stellarators. However, while the associated plasma cooling cannot be recovered as may happen in stellarators [32], an important point in RFX-mod is that the onset of the thermal instability does not end disruptively, as might happen in tokamaks: a soft landing of the plasma discharge is observed.

5. Edge turbulence properties and transport

5.1. Momentum transport and flow profile at the edge.
Plasma flow profile has been measured at the edge of low-current RFX-mod plasma with two
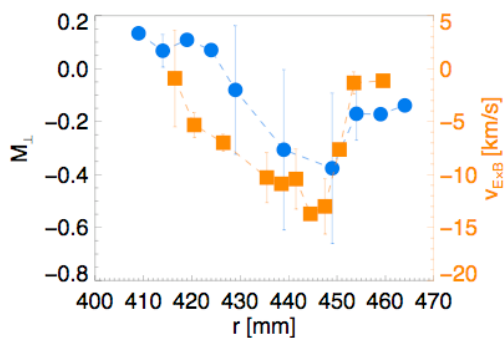

Fig. 10: perpendicular Mach number and radial $E \times B$ velocity profiles at the RFX-mod edge

kinds of insertable probes [11]. The typical perpendicular (toroidal) plasma flow profiles are shown in Fig. 10. The graph displays the Mach number, that is the plasma velocity normalized to the ion sound speed. As in the old RFX [33], the perpendicular velocity displays a double shear: a first shear region is located across the $r = a$ surface, whereas a second shear is found deeper into the plasma. For comparison, in the same figure the radial $E \times B$ velocity profile obtained in another set of discharges is shown. The two profiles display a quite good agreement, taking into account possible toroidal asymmetries and slightly different discharge conditions. Electrostatic fluctuations play a fundamental role in driving the edge flow. The toroidal component of the edge turbulence propagation velocity v_ϕ is given also by the Gas Puffing Imaging diagnostic [34]. There is evidence of toroidal propagation of emission bursts in the same direction as the $E \times B$ drift flow [35]. The fluctuation velocity has been found in the past to be experimentally consistent, both in direction and absolute value, with the $E \times B$ drift obtained from the radial gradient of plasma potential [36]. This velocity changes with the Greenwald density, n/n_G: it is higher at lower density, and then decreases, reaching a saturation level of 15 km/s at $n/n_G \approx 0.35$.

5.2 Coherent turbulent structures and transport at the plasma edge
Understanding and controlling the mechanism driving anomalous transport is a key issue for fusion experiments. Experimental observations performed in tokamaks, stellarators, RFPs and linear devices [37] have revealed the intermittent nature common to plasma turbulence, and the fact that intermittency is generally associated to the presence of "blobs", that is coherent structures, which have been identified as vortices [38]. These structures are the results of strong non-linearities: they are now generally described as 3-d features elongated in the parallel direction.

Measurements of different electrostatic quantities [11] have been analyzed to identify coherent structures associated to strong bursts in the fluctuation time series. Peaks on the electron pressure signal have been used as trigger. The average features of these events have then been extracted by applying the conditional average. The typical coherent structure detected by this method at the scale $\tau = 3.3$ μs is shown in Fig. 11. A parallel vorticity peak accompanies the pressure peak, so that it can be deduced that the pressure structure is associated to a local velocity eddy.

Fig. 11-c displays the parallel current density, deduced computing the parallel component of $\nabla \times \mathbf{B}$. A clear relation exists between the pressure structures and a parallel current density peak. The other two components of the current density are one order of magnitude smaller, so that the pressure blobs are associated to a current filament parallel to the local magnetic field. Recent work has identified these electromagnetic coherent structures as Drift Kinetic Alfvén vortices [38]. This kind of structures has been detected in the Earth's ionosphere, and in RFX-mod for the first time in a laboratory plasma.
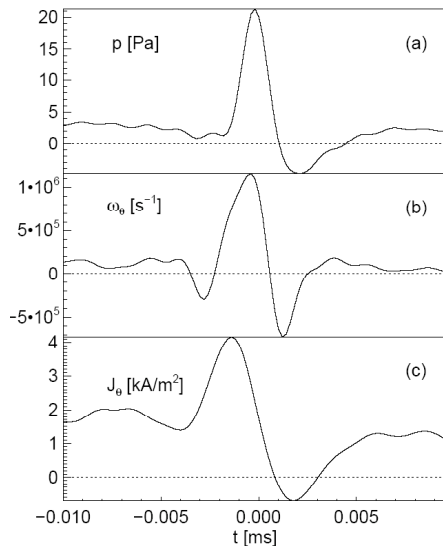

Fig. 11: Typical coherent structure as seen on pressure, parallel vorticity and parallel current density at the scale $\tau = 3.3$ μs.

In presence of coherent structures the plasma diffusion coefficient can be separated in a part due to the plasma trapped in coherent structures D_p and another one due to the background uncorrelated turbulence, usually set equal to the Bohm diffusion [39]. D_p scales with the normalized density n/n_G. and its average value displays a decrease of about a factor 2 between discharges with low and high value of n/n_G. This result can be discussed in terms of an increase of blob viscous damping at higher n/n_G values, though further investigation are underway.

6. Conclusions

Very good progress in performance, physics understanding and technology has been achieved in RFX-mod since the last Fusion Energy Conference in 2006. The reliable access to high current, above 1 MA, has revealed a new self-organized regime, where the confinement performance is significantly improved and transport barriers are observed. The RFP dominated by magnetic chaos belongs to the past, and the new findings open an exciting and clear path. On the basis of the present results and of the machine technical capabilities, this path deserves to be explored and it is expected to lead to even better performance.

The achievements in the field of MHD stability physics and real-time control have been numerous and of high quality. Progresses in control of tearing modes and RWM have been reported. Besides providing an improved magnetic boundary for the high current operation, the feedback experiments address general issues like multi-mode control, tools for mode unlocking and for forcing mode rotation, implementation of advanced control theory, development of a robust plant model including features of the plasma, wall, sensors, actuators, field error environment, noise environment and controller dynamics, incorporation of 3-d effects due to a non-axisymmetric wall, numerical codes benchmarking; study of situations with a downgraded set of coils are planned to address the effects of a non-complete coil coverage, which is the standard situation in tokamak.

All these results, together with a big effort on education and training, give a strong confidence in the RFX-mod future activities and reinforce its integration in the European and international fusion programme.

REFERENCES

[1]   SONATO P. et al. Fusion Eng. Des. **66 (**2003) 161
[2]   LUCHETTA A. et al., 21th IAEA Fus. Energy Conf., Chengdu, China, (2006), paper FT/P5-1
[3]   ESCANDE D.F. et al., Phys. Rev. Lett. **85**, 1662 (2000)
[4]   BISHOP C.M., Plasma. Phys. Control. Fusion. **31** 1179 (1993)
[5]   MARTINI S. et al., 21th IAEA Fus. Energy Conf., Chengdu, China, (2006), paper EX/P7-3
[6]   PACCAGNELLA R. et al., (2006) Phys Rev. Lett. **97** 075001
[7]   PACCAGNELLA R. et al. Nucl. Fusion 42 (2002) 1102–1109
[8]   ZANCA P. et al. , Nucl. Fusion, **47** (2007) 1425
[9]   MARRELLI L. et al., "Active Control of Resistive kink-tearing modes in RFX-mod", (2008), this conference, paper EX/P9-8
[10]   LUCHETTA A. et al., "Technology Progress in real-Time Control of MHD Modes at RFX-mod", this conference, paper FT/P2-20
[11]   MARTINES E. et al., "Transport Mechanisms in the Outer Region of RFX-mod", this conference, paper EX/P5-26
[12]   DRAKE J.R. et al, "Reversed-Field Pinch Contributions to Resistive Wall Mode Physics and Control", this conference, paper EX/P9-7
[13]   BOLZONELLA T. et al., "Resistive Wall Mode Active Rotation in RFX-mod", (2008) accepted for publication in Phys. Rev. Lett.
[14]   LA HAYE R. J. et al., Nucl. Fusion **44**, 1197 (2004).
[15]   REIMERDES H. et al., Phys. Rev. Lett. **98**, 055001 (2007).
[16]   TAKECHI M. et al., Phys. Rev. Lett. **98**, 055002 (2007).
[17]   VILLONE, F. et al., 34th EPS Conf. on Plasma Phys. Warsaw, ECA Vol.31F, P-5.125 (2007)
[18]   VILLONE F. et al., Phys. Rev. Lett. **100**, 255005 (2008)
[19]   SOPPELSA A. et al. Fusion Engineering and Design **83** (2008) 224–227
[20]   SOPPELSA A. et al., "Integrated identification of RFX-mod active control system from experimental data and finite element model", to be published in Proc. 2008 Symposium on Fusion Technology – SOFT – Rostock, (2008).
[21]   VALISA M. et al., "High current operation in RFX-mod", accepted for publication in Plasma Phys. Contr. Fusion (2008)
[22]   CAPPELLO S. and ESCANDE D.F., Phys. Rev. Lett. **85**, 3838 (2000)
[23]   ESCANDE D.F. et al.,Phys. Rev. Lett. **85**, 3169 (2000)
[24]   LORENZINI R. et al., Phys. Rev. Lett. 101, 025005 (2008)
[25]   CARRARO L. et al., "Improved Confinement with Internal Electron Transport Barriers in RFX-mod", this conference, paper EX/P3-9
[26]   MARTINES E. et al., private communication, manuscript in preparation
[27]   GUO S.C., submitted to Phys. Rev. Lett. (2008)
[28]   GARBET X. et al   Phys. Rev. Lett. **91** 035001 (2001)
[29]   KOTSCHENREUTHER M. et al Comput. Phys. Commun. 88   128 (1995)
[30]   INNOCENTE P., et al., ., 21th IAEA Fus. Energy Conf., Chengdu, China, (2006), paper EX/P3-10
[31]   PUIATTI M.E. et al., "High density physics in Reversed Field Pinches: comparison with Tokamaks and Stellarotors", this conference, paper EX/P5-05
[32]   WOBIG H, Plasma Phys. Contr. Fus. **42** (2000) 931
[33]   ANTONI V. et al., Phys. Rev. Lett. **79** (1997) 4814.
[34]   AGOSTINI M. et al., Rev. Sci. Instrum. **77** (2006) 10E513.
[35]   SCARIN P. et al., J. Nucl. Mater. **363-365** (2007) 669.
[36]   ANTONI V. et al., J. Nucl. Mater. **313-316** (2003) 972.
[37]   SERIANNI G. et al., Plasma Phys. Control. Fusion **49** (2007) B267.
[38]   VIANELLO N. et al., "Observation of drift-kinetic-Alfvén vortices in laboratory plasmas" (2008), submitted to *Nature Physics*.
[39]   HORTON W. and ICHIKAWA Y. H., *Chaos and Structures in Nonlinear Plasmas* (World Scientific, Singapore, 1996)